

# Thermal challenges in MEMS applications: phase change phenomena and thermal bonding processes

Liwei Lin\*

*Department of Mechanical Engineering, University of California at Berkeley, 5126 Etcheverry Hall, MC 1740, Berkeley, CA 94720, USA*

## Abstract

Two thermal challenges for current and next generation microelectromechanical systems (MEMS) applications are discussed. The first topic is the fundamental investigations of phase change phenomena in the microscale. It has been demonstrated that microresistive heaters can generate single, spherical and controllable thermal bubbles with diameters between 2 and 500  $\mu\text{m}$ . Both simplified steady state and transient analyses that provide the scientific foundation of bubble nucleation in the microscale have been established but require further investigations. Several device demonstrations are briefed including microbubble-powered actuators, microbubble-powered nozzle-diffuser pumps and microbubble-powered micromixers for applications in microfluidic systems. The second topic addresses key heat transfer issues during the thermal bonding processes for MEMS fabrication and packaging applications. Basic thermal analyses on the microscale bonding processes have been developed while in-depth study is required to advance the understandings of the thermal bonding processes in the microscale. Successful new thermal bonding processes are introduced, including localized eutectic bonding, localized fusion bonding, localized chemical vapor deposition (CVD) bonding, localized solder bonding and nanosecond laser bonding for encapsulation of MEMS devices.

© 2003 Elsevier Science Ltd. All rights reserved.

*Keywords:* Bubble; Phase change; Thermal bonding; Microelectromechanical systems

## 1. Introduction

Challenging thermal problems emerge as the size of micromechanical devices is shrinking in microelectromechanical systems (MEMS) or nanoelectromechanical systems (NEMS) applications. In the past 20 years, the application of microelectronic technology to the fabrication of mechanical devices stimulated various research directions in semi-conductor microsensors and microactuators. Micromachining technologies take the advantage of batch processing to address the manufacturing and performance requirements of the sensor industry. The versatility of semiconductor materials and the miniaturization of VLSI patterning techniques promise new sensors with better capabilities and improved performance-to-cost ratio over those of conventionally machined devices. Furthermore, the shrinking of device size results in increasing surface-to-volume ratio. As a result, new devices and new manufacturing processes that were viewed as impossible previously in the macro world become feasible in the microscale.

In the area of heat transfer related topics, for example, two categories of thermal phenomena/processes and their future challenges are discussed in this paper. The first one deals with microbubble-powered actuators utilizing phase change from liquid to vapor phases in the microscale and its applications to microdevices. These actuators have distinct advantages over other types of actuation sources in the microscale due to operation at low voltage, easy implementation by introducing resistive heaters, and no moving mechanical structures. Although the boiling process is routinely observed in our daily life, the generation and control of a single thermal bubble can only be accomplished in the microscale and this new phenomenon opens up many possible applications. Due to the high surface-to-volume ratio in the microscale, heating sources can be applied using tiny volumetric heat generation and the generated heat flux can be balanced by the surface condensation of the vapor bubble. When the overall heat transfer process consisting of heat generation, condensation and heat losses to the environment reaches equilibrium, thermal bubbles becomes controllable [1]. In an effort to understand bubble formation processes in the microscale, the transient behavior of the phase change phenomena on microheaters has been investigated [2]. These fundamental studies help

\* Tel.: +1-510-643-5495; fax: +1-510-643-5599.

E-mail address: [lwlin@me.berkeley.edu](mailto:lwlin@me.berkeley.edu) (L. Lin).

the successful development of new microbubble devices, including bubble-powered mechanical actuators [3], bubble-powered nozzle-diffuser pumps [4] and bubble-generated mixing effects [5]. Although the proof-of-principle microdevices have been demonstrated, more scientific challenges have to be addressed before optimizations of these devices or new microdevices can be envisioned.

The second microscale thermal challenge is in the thermal bonding process by using selective and localized heating. In the microscale bonding process, the primary goal is to establish strong bonding with minimum thermal budget to reduce possible thermal damages to existing materials that were already placed on the wafer. This requirement happens often in the packaging of MEMS devices that a good hermetic sealing is required but existing MEMS materials or microelectronics cannot be damaged during the bonding process. Again, the increase of volumetric heat generation rates and surface heat fluxes make several new thermal bonding process possible. Localized heating provides the key advantage by utilizing thermal management schemes in the microscale to minimize the thermal budget and thermal damages since the energy is provided locally. At the same time, the bonding strength is maximized because the processing temperature can be adjusted to be very high locally to supply the bonding energy. Several successful bonding schemes have been developed and will be discussed, including the localized eutectic bonding process [6], localized fusion bonding process [7], localized solder bonding process [8], localized chemical vapor deposition (CVD) bonding process [9] and nanosecond laser welding process [10].

## 2. Phase change phenomena in the microscale

Phase change phenomena can be applied in the microscale as the actuation mechanism by simply using the method of resistive heating. In several previous publications [1–5], resistive heaters are made of either heavily phosphorus doped polysilicon or metal layers with a thickness between 100 nm and 2  $\mu\text{m}$ . The width of these microheaters varies from 1 to 10  $\mu\text{m}$  and the length ranges from 50 to 1000  $\mu\text{m}$ . The following discussions start with the fundamental investigations of phase changes processes and continue with examples of successful device demonstrations.

### 2.1. Fundamental studies

#### 2.1.1. Phase change and bubble formation

Microheaters have been designed and fabricated by using a standard micromachining process [11]. A one-dimensional microheat transfer model was established based on the conservation of energy to estimate the temperature distribution on the microheater [12]. For example, Fig. 1 shows

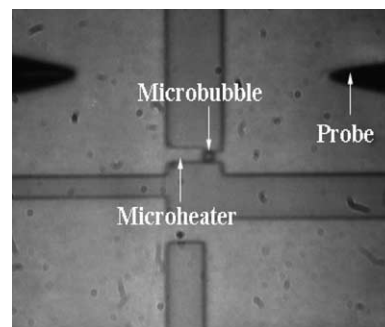


Fig. 1. A single thermal bubble of 2  $\mu\text{m}$  in diameter is generated on a microresistive heater immersed in Fluorinert liquid [1].

a 15  $\mu\text{m}$  long, polysilicon microheater of two widths: 3  $\mu\text{m}$  wide on the left 10  $\mu\text{m}$  region and 2  $\mu\text{m}$  wide on the right 5  $\mu\text{m}$  portion. It was placed in a pool of electrically inert liquid of Fluorinert at room temperature. When the heater is resistively heated by passing an electrical current, the temperature distribution was uneven and nonlinear as predicted by using the one-dimensional thermal model. The highest temperature occurs at the place that the thermal bubble was attached to as shown in Fig. 1 due to the Marangoni effect. Experimentally, individual, spherical vapor bubbles with diameters of 2–500  $\mu\text{m}$  have been generated with stable and controllable characteristics. Although initial thermal analyses were developed, including Hsu's analysis and the conservation of energy to explain possible microbubble formation mechanisms [1], further studies are required for better understanding of the phase change phenomena in the microscale. Challenges and possible directions are: in situ and remote temperature measurements at various locations of the microresistive heater during the bubble formation process; models describing bubble incipience mechanisms by using microheaters and under sub-cooled boiling conditions; transport and the dynamic equilibrium processes of vaporization and condensation of a single thermal bubble for controllable bubble growth; and three-dimensional thermal and fluidic analyses on the incipient and growth stages of the microbubble formation processes [13].

#### 2.1.2. Transient phase change behavior

The characterizations of transient phase change phenomena in the microscale were conducted afterwards. It has been discovered that transient temperature responses can be classified into three groups by the level of input currents as shown in Fig. 2 [2]. When the input current level is low, the wall temperature stays nearly constant and no bubble is generated. When the input current is set to be above a critical level, the wall temperature increases initially, quickly drops afterwards until a bubble is nucleated, and rises afterwards until steady state is reached. In the third group that has a high input current level, the wall temperature rises sharply as soon as the current is applied and a bubble is formed immediately. Overall, a major

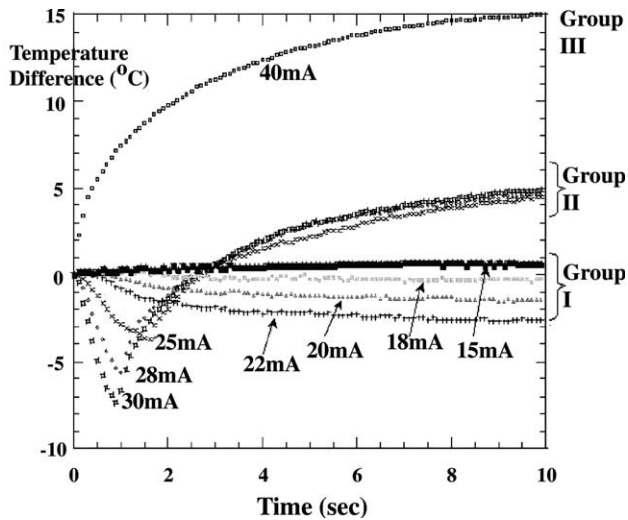


Fig. 2. Transient bubble formation experiments showing three groups of bubble formation characteristics [2].

difference between micro- and macroscale boiling experiments is observed in the second group of experiments when the wall temperature drops before the nucleation of a microbubble. Theoretical models have been established to estimate the temperature of microheater during the transient phase change process [2]. The time constant of the resistor was calculated in the microsecond range and that for the silicon substrate was calculated in the millisecond range. Although this transient phase change analysis only covered several basic parameters, it provided interesting and important foundations for future studies. Many challenging problems on the transient behavior of phase change phenomena in the microscale are: analytical models to characterize the three groups of transient bubble formation phenomena, the growth rate of the thermal bubble with respect to various input power and time and the transient stage of evaporation and condensation process, transient behavior of bubble formation in extremely short periods such as microseconds, and the effects of substrate and environment to the heat conduction cooling process for high speed and better bubble nucleation.

## 2.2. Applications

The demonstration of phase change phenomena by using microresistive heaters led to the successful implementation of several new microfluidic devices. These applications are different than the well-known bubble jet printers [14] but have great potential as successful commercial products as demonstrated by bubble jet printers taking of the advantages of low driving voltage, easy implementation, and the precise and miniaturized actuation mechanism.

### 2.2.1. Microbubble-powered mechanical actuators

Micromechanical actuators based on the actuation of thermal bubbles have been demonstrated [3]. The schematic

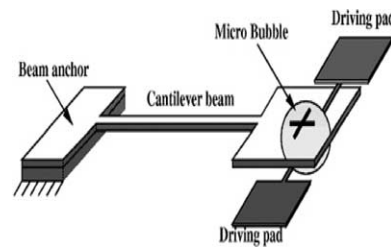


Fig. 3. Schematic illustration of a microbubble powered actuator [3].

diagram of the device is shown in Fig. 3 by using the surface micromachining process [11] to fabricate both the polysilicon resistor as microheater and cantilever-type actuator. The heavily phosphorus doped polysilicon resistor worked as the resistive microheater to generate controllable thermal bubbles directly underneath the actuator plate with either AC or DC inputs to push and control the height of the actuator. A maximum vertical deflection of  $140\ \mu\text{m}$  and a maximum force of  $2\ \mu\text{N}$  have been achieved. This new class of actuator has potential applications as a flow regulator to control microfluidic systems, a reflector in an optical system, or a relay in an electrical control system. Challenging thermal issues have been identified before the performance and controllability of the device can be improved. These include a three-dimensional local temperature profile analysis, the transient responses when the thermal bubble is in contact with the mechanical constraint, and the mechanical pressure–force relationship in conjunction with the thermal bubble geometry under the influence of the actuator plate.

### 2.2.2. Microbubble-powered nozzle-diffuser pumps

Thermal bubble-powered pumps with the design of a pair of nozzle-diffuser flow regulator have been successfully demonstrated [4]. The valve-less pump consists of a meander resistive heater, a pair of nozzle-diffuser flow controller, and a 1 mm in diameter,  $50\ \mu\text{m}$  in depth pumping chamber as shown in Fig. 4. Microthermal bubbles were generated by electrical power inputs at a frequency up

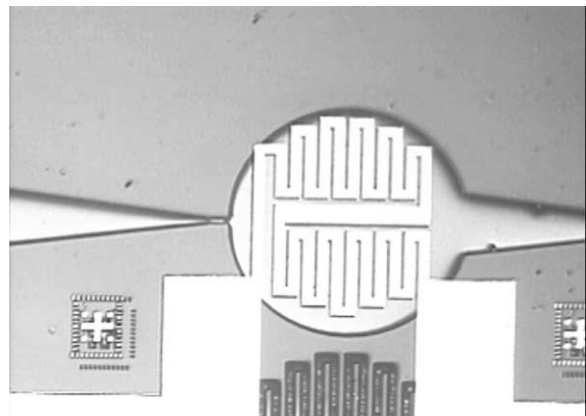


Fig. 4. A fabricated microbubble-powered nozzle-diffuser pump. The metal heater is built on a glass wafer that is transparent for the viewing of the pumping operations [4].

to 500 Hz. Periodically expanding and collapsing thermal bubbles actuated liquid flows back and forth and the nozzle and diffuser design generates a net liquid flow from the nozzle to the diffuser side. The measured pumping flow rate by using IPA fluid can go up to 5  $\mu\text{l}/\text{min}$  and the highest pumping pressure was 377 Pa with a power consumption of about 0.5 W as shown in Fig. 5 [4]. The experimental results were compared with a similar pump design driven by piezoelectric actuator that the pumping rate increased as the driving frequency increased initially and decreased at higher pumping frequency when the piezoelectric pumping stroke decreased [15]. In the bubble-powered micropump, the pumping rate increased as the driving frequency increased initially but reduced at higher frequency when residual bubbles piled up in the actuation chamber and reduced the pumping pressure. The challenges here appear to be the optimization of the pump design in order to reduce the residual bubbles and to increase the flow rate and pumping pressure. These will require investigations in the heat transfer process during the periodically nucleating and collapsing thermal bubbles, the flow patterns and pressure head induced by the thermal bubbles and various designs of the nozzle-diffuser pair. Furthermore, temperature is the big concern in the application of these thermal bubble pumps to biological system and a good thermal analysis can predict the percentage of liquid under high temperature treatment and can determine the feasibility of the specific application.

### 2.2.3. Microbubble-powered mixers

A microfluidic mixer powered by the bubble pump has been demonstrated [5]. The device can accelerate the mixing process in the microscale by using the generated oscillatory flow to induce wavy flow interfaces to increase the contact area of the mixing liquids. It was found that the mixing effect could be optimized when the pumping frequency reaches 200 Hz in a 200  $\mu\text{m}$  wide, 5  $\mu\text{m}$  deep microchannel with a pumping volume flow rate of 6.5  $\mu\text{l}/\text{min}$ . When the length of the mixing wave is shorter than

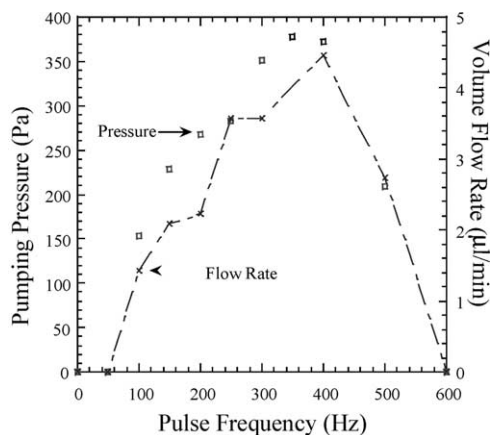


Fig. 5. Pumping pressure at zero flow rate and volume flow rate at zero back pressure of the microbubble-powered nozzle-diffuser pump under a 5% pulse duty and 0.5 W average input power [4].

the diffusion length of the mixing fluids, the mixing effect is optimized and this can be accomplished by adjusting the pulse frequency until the optimal mixing effect is achieved. Experimentally, normalized gray-scale values corresponding to the mixing effect increased proportionally to the one-third power of the pumping pulse frequency. However, the fundamental explanation does not exist due to the lack of a good analytical model in predicting and verifying experimental data. This would be a challenging and interesting problem dealing with combined domains of thermal and fluidic regions.

### 2.2.4. Other applications

Many liquid-to-vapor phase change devices have been proposed over the past years. The most famous one is the bubble-jet printer that uses phase change phenomena to eject ink droplets [14]. In a previous review paper [13], an electric-to-fluidic membrane valve [16], a microsteam engine using thermal bubbles as the power source [17], bubble formation inside confined microchannels for applications as a valve or pump [18,19], bubble generation as a planar laminar mixer [20] and a light driven micropump [21] were reviewed. Additional applications have been presented in recent years such as using thermal bubble as a bio-particle actuator [22], in a transdermal bio-molecular patch [23]. All of these devices take the advantages of easy implementation, manufacturing and generation of the phase change mechanism in the microscale. However, except the bubble-jet printer, there are very few fundamental studies in other applications. It is important to establish analytical models, numerical simulation tools and experimental protocols for the phase change phenomena in the microscale before these potential applications can be fully realized and become commercial products.

## 3. Thermal bonding processes in the microscale

### 3.1. Fundamentals

The development of thermal bonding processes is motivated by the fabrication and packaging needs for MEMS devices. In conventional IC industry, up to 95% of the manufacturing cost may be attributed to the packaging processes and the cost of packaging may go even higher for MEMS devices due to the stringent packaging requirements for microstructures. In the past, anodic bonding [24], fusion bonding [25], reactive gas sealing [26] and LPCVD sealing [27] processes have been used to encapsulate MEMS devices. However, none of them are suitable for the general purpose of MEMS packaging processes at low temperature and at low cost. Therefore, a new wafer-level packaging approach that is insensitive to the MEMS fabrication processes is proposed based on the principle of localized heating and bonding as shown in Fig. 6 [28]. The basic idea is to increase the thermal bonding temperature locally but to

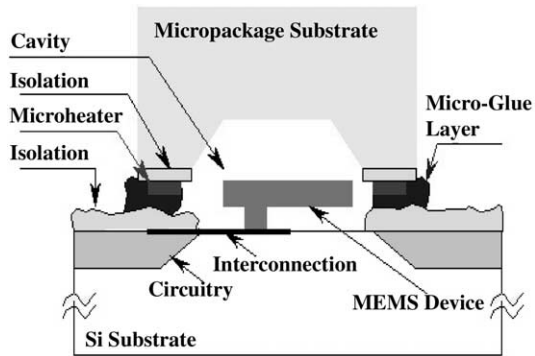


Fig. 6. The schematic diagram showing the principle of localized heating and bonding processes for MEMS packaging and fabrication applications. The bonding energy is locally generated such that the global temperature at the wafer-level can be kept low during the bonding process [28].

keep the temperature low at the wafer level. As a result, high energy is supplied for strong bonding locally and low temperature environment is maintained at the wafer-level. Several new localized bonding processes are proposed and demonstrated.

### 3.2. Applications

#### 3.2.1. Localized eutectic, fusion and solder bonding

The localized heating and bonding principle is first applied to conventional thermal bonding processes, including eutectic, fusion and solder bonding. In the localized eutectic bonding process, the silicon–gold system has been adopted for the demonstration because it can provide high bonding strength and good stability at a relatively low processing temperature (about 363 °C). Experimentally, heating was achieved by applying a DC current through micromachined heater made of gold that serves as both the heating and bonding material. At the interface of silicon and gold, the formation of eutectic bond took place in about 5 min [6]. After the bond was forcefully broken as shown in Fig. 7, the fracture and separation occurred either in the bulk

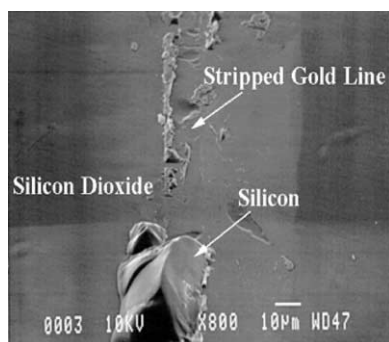


Fig. 7. A SEM microphoto showing the gold microheater after forcefully breaking the silicon–gold eutectic bond that was formed by using the localized heating method. The strength of the bond is comparable with the fracture toughness of the bulk silicon such that the fracture and separation occur either in the bulk silicon or at the gold–silicon dioxide interface [6].

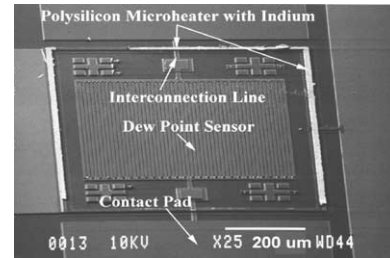


Fig. 8. A SEM micrograph of silicon substrate with a dew point sensor after breaking the indium–glass bond. The sensor is designed to monitor the hermeticity of the package [8].

silicon or at the gold–silicon dioxide interface. Therefore, it can be concluded that the bonding strength was as strong as the silicon fracture toughness.

The same scheme has been applied to the localized silicon-to-glass fusion bonding process with successful results. Moreover, the polysilicon-to-glass bonding activation energy was measured as 1.6 eV and this number is close to those from silicon-to-glass direct bonding [7]. The third localized heating and bonding scheme is to use metal solder in the bonding process. For example, a dew point sensor is designed and to be packaged inside the bonding cavity as shown in Fig. 8. The bonding solder is indium and the bonding system is indium-to-glass. A glass cap wafer is placed on top and sealed by localized heating and bonding and the dew point sensor is used to monitor the leakage of the package [8]. Several other solder-based bonding systems have been used, such as aluminum–glass and aluminum/polysilicon–glass system with improved results [29]. The advancement of this approach also includes a vacuum encapsulated micromechanical polysilicon resonators with quality factor as high as 9000 [30].

In general, thermal challenge issues for localized heating and bonding processes comes from the existence of a strong local temperature gradient. As a result, several thermal related issues have to be reconsidered, for example, the residual thermal stress generated during the bonding process, the diffusion of bonding solders, and the localized melting and solidification processes when the bonding solders are melted and solidified. Because both the solid-to-liquid and liquid-to-solid phase change processes may be involved, it is very challenging to establish an analytical model and simulation tool to describe and predict the various localized heating and bonding processes.

#### 3.2.2. Localized CVD bonding

The localized CVD process is conducted by selectively growing polysilicon on a microheater in a low vacuum, silane environment. Experimental results showed that silane would decompose at an elevated temperature of more than 500 °C to form polysilicon locally on the microheater in contrast to the global CVD process that would have polysilicon grown on the whole substrate. The top figure in Fig. 9 is the electro-thermal simulation result (top) of

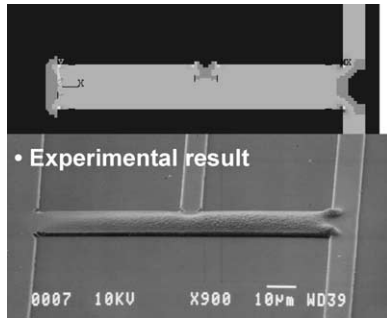


Fig. 9. (Top) Temperature simulation of a microheater under a current input. Hot spots can be identified. (Bottom) CVD polysilicon is deposited following the temperature distribution and surface-reaction limited process is identified.

the temperature distribution when an input current is applied to the experimental sample. The bottom photograph is the deposition profile. It is observed that the thickness of the deposited film seems to follow the temperature profile such that surface-reaction limited process is identified as the deposition process. This localized CVD process is applied to MEMS packaging to selectively encapsulate MEMS devices. It is found that an area of  $1000 \times 800 \mu\text{m}^2$  can be enclosed under one hour of the localized CVD process by filling up a gap of about  $1 \mu\text{m}$  between the microheater and a top capping substrate [9]. This process is believed to be applicable for MEMS packaging and fabrication with the advantage of excellent bonding strength and low temperature processing at the wafer-level. Many thermal challenges have to be addressed before the process can be optimized. These will include thermal and fluidic analyses on the deposition gas flowing into the thin gap and the decomposition reaction inside the small cavity before and during the sealing process, the chemical vapor reaction during the deposition process under a strong local temperature gradient and other issues that may involve thermal analyses, gas flow as well as decomposition, recombination and solidification of materials in the microscale.

### 3.2.3. Localized nanosecond laser bonding

In another effort to achieve localized heating and bonding, a nanosecond-pulsed laser bonding process with a built-in mask for MEMS packaging application has been successfully demonstrated. A YAG Surelit II laser with pulse duration of 4–6 ns, a wavelength of 355 nm and a focal diameter of 1 mm is used to provide the bonding energy for glass-to-silicon bonding with a  $4 \mu\text{m}$  thick indium as the intermediate bonding layer. The optimal bonding parameter was found experimentally when the laser energy is between 8 and 22 mJ and multiple laser shots were used [10]. With the assistance of a regular paper as the masking material with predefined patterns such as a ring as shown in Fig. 10, localized and selective heating and bonding can be achieved as shown in the bottom microphoto in Fig. 10. In addition to the thermal challenges suggested in

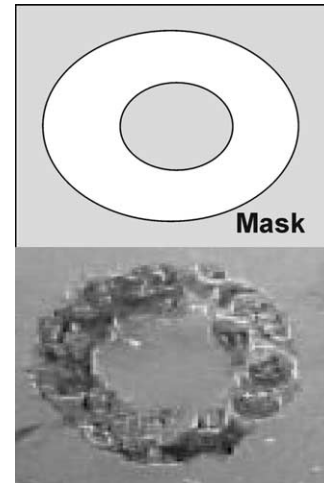


Fig. 10. Nanosecond laser bonding with a built-in mask with (top) the mask and (bottom) the bonding result of indium to glass bond [10].

the above sections, ultra fast laser bonding presents interesting issues in the time domain analyses and experiments for the control and verification of experimental results. Furthermore, the thermal problem of laser absorption at the mask, the proper masking material selection as well as the heat transfer processes dealing with heat conduction and phase change in such a small time and space scale may present interesting challenges.

## 4. Conclusions

Thermal challenges in the area of phase change phenomena and thermal bonding processes in the microscale have been discussed. Although many interesting thermal challenges have been raised and some initial works have been conducted in issues related to these areas, it should be noted that these two subjects are merely two of the many scientific challenges in the microscale. There are plenty of rooms and fruitful of research directions in microscale thermal sciences that should be vigorously pursued. Another important observation as demonstrated by the above examples is that microscale thermal challenges will often combine with issues from other domains such as fluidic problems that have to be dealt with simultaneously and cannot be overlooked.

## Acknowledgements

The author would like to thank Drs J.H. Tsai, Y.T. Cheng, G.H. He and C. Luo for contributions in several of the experiments presented in this paper. This work is supported in part by an NSF Career (ECS-0096098) award and a DARPA/MTO/MEMS grant.

## References

- [1] L. Lin, A.P. Pisano, V.P. Carey, Thermal bubble formations on polysilicon micro resistors, *ASME J. Heat Transfer* 120 (September) (1998) 735–742.
- [2] H. Tsai Jr., L. Lin, Transient thermal bubble formation on polysilicon micro resistors, *ASME J. Heat Transfer* 124 (2) (2002) 375–382.
- [3] L. Lin, A.P. Pisano, Thermal bubble powered microactuators, *Microsyst. Technol. J.* 1 (1) (1994) 51–58.
- [4] H. Tsai Jr., L. Lin, A thermal bubble actuated micro nozzle-diffuser pump, *IEEE/ASME J. Microelectromech. Syst.* 11 (2002) 665–671.
- [5] H. Tsai Jr., L. Lin, Active microfluidic mixer and gas bubble filter driven by thermal bubble micropump, *Sens. Actuators, A* 97–98 (2002) 665–671.
- [6] L. Lin, Y.T. Cheng, K. Najafi, Formation of silicon–gold eutectic bond using localized heating method, *Jpn. J. Appl. Phys., Part II* 11B (November) (1998) 1412–1414.
- [7] Y.T. Cheng, L. Lin, K. Najafi, Localized silicon fusion and eutectic bonding for MEMS fabrication and packaging, *IEEE/ASME J. Microelectromech. Syst.* 9 (March) (2000) 3–8.
- [8] Y.T. Cheng, L. Lin, K. Najafi, A hermetic glass–silicon package formed using localized aluminum/silicon–glass bonding, *IEEE/ASME J. Microelectromech. Syst.* 10 (3) (2001) 392–399.
- [9] G.H. He, L. Lin, Y.T. Cheng, Localized CVD bonding for MEMS packaging, 10th International Conference on Solid State Sensors and Actuators, Transducer's 99, Technical Digest, Sendai, Japan, June 1999, pp. 1312–1315.
- [10] C. Luo, L. Lin, The application of nanosecond-pulsed laser welding technology in MEMS packaging with a shadow mask, *Sens. Actuators, A* 97–98 (2002) 398–404.
- [11] D. Koester, R. Majedevan, A. Shishkoff, K. Marcus, Multi-User MEMS Processes (MUMPS) Introduction and Design Rules, rev. 4, MCNC MEMS Technology Applications Center, Research Triangle Park, July 1996, NC 27709.
- [12] L. Lin, Selective encapsulations of MEMS: micro channels, needles, resonators and microelectromechanical filters, PhD Dissertation, Mechanical Engineering Department, University of California, Berkeley, 1993.
- [13] L. Lin, Microscale thermal bubble formation: thermophysical phenomena and applications, *Microscale Thermophys. Engng* 2 (2) (1998) 71–85.
- [14] N.J. Nielsen, History of thinkjet printerhead development, *HP J.* 36 (5) (1985) 4–10.
- [15] A. Olsson, G. Stemme, E. Stemme, A valveless planar fluid pump with two pump chambers, *Sens. Actuators, A* 46–47 (1995) 549–556.
- [16] M.J. Zdeblick, J.B. Angell, A microminiature electric-to-fluidic valve, International Conference on Solid State Sensors and Actuators, Transducer's 87, Technical Digest, 1987, pp. 827–829.
- [17] J.J. Sniegowski, A micro actuation mechanism based on liquid–vapor surface tension, International Conference on Solid State Sensors and Actuators, Transducer's 93, Late News Technical Digest, 1993, pp. 12–13.
- [18] L. Lin, K.S. Udell, A.P. Pisano, Vapour bubble formation on a micro heater in confined and unconfined micro channels, *Thermal Sci. Engng* 2 (1) (1994) 52–59.
- [19] T.K. Jun, C.-J. Kim, Microscale pumping with transversing bubbles in microchannels, Proceedings 1996 Solid-State Sensors and Actuators Workshop, Hilton Head, SC, 1996, pp. 144–147.
- [20] J. Evans, D. Liepmann, A.P. Pisano, Planar laminar mixer, Proceedings of IEEE Micro Electro Mechanical Systems Conference, January 1997, pp. 96–101.
- [21] H. Mizoguchi, M. Ando, T. Mizno, T. Takagi, N. Nakajima, Design and fabrication of light driven micropump, Proceedings of IEEE Micro Electro Mechanical Systems Conference, January 1992, pp. 31–36.
- [22] R.A. Braff, et al., A microbubble-powered bioparticle actuator, Solid-State Sensor and Actuator Workshop, Hilton Head, 2002, pp. 138–141.
- [23] M. Paranjape, et al., Dermal thermo-poration with a PDMS-based patch for transdermal biomolecular detection, Solid-State Sensor and Actuator Workshop, Hilton Head, 2002, pp. 73–76.
- [24] G. Wallis, D. Pomerantz, Filed assisted glass–metal sealing, *J. Appl. Phys.* 40 (1969) 3946–3949.
- [25] K.E. Peterson, P. Barth, et al., Silicon fusion bonding for pressure sensors, 1988 Solid-State Sensor and Actuator Workshop, Hilton Head, 1988, pp. 144–147.
- [26] J.J. Sniegowski, H. Guckel, R.T. Christenson, Performance characteristics of second generation polysilicon resonating beam force transducers, IEEE Solid-State Sensor and Actuator Workshop, Hilton Head Island, 1990, pp. 9–12.
- [27] L. Lin, R.T. Howe, A.P. Pisano, Microelectromechanical filters for signal processing, *IEEE/ASME J. Microelectromech. Syst.* 7 (September) (1998) 286–294.
- [28] L. Lin, MEMS Post-packaging by localized heating and bonding, *IEEE Trans. Adv. Packag.* 23 (November) (2000) 608–616.
- [29] Y.T. Cheng, L. Lin, K. Najafi, A hermetic glass–silicon package formed using localized aluminum/silicon–glass bonding, *IEEE/ASME J. Microelectromech. Syst.* 10 (3) (2001) 392–399.
- [30] Y.T. Cheng, W.T. Hsu, K. Najafi, C.T. Nguyen, L. Lin, Vacuum packaging technology using localized aluminum/silicon-to glass bonding, *IEEE/ASME J. Microelectromech. Syst.* 11 (2002) 556–565.